Effects Of Three-Dimensional Conducting Structures On Resistive Wall Modes

Fabio Villone[a], Yueqiang Liu[b], G. Ambrosino[c] and A. Pironti[c]

[a] *Ass. Euratom/ENEA/CREATE, DAEIMI, Università di Cassino*
Via Di Biasio 43, 03043, Cassino (FR), Italy
[b] *EURATOM/UKAEA Fusion Association*
Culham Science Centre, Abingdon, OX14 3DB, UK
[a] *Ass. Euratom/ENEA/CREATE, DIS, Università di Napoli Federico II*
Via Claudio 21, 80125, Napoli, Italy

Abstract. This paper illustrates the effect of three-dimensional conducting structures on the evolution of Resistive Wall Modes (RWM) occurring in toroidal fusion devices. The CarMa code is used to derive the model, which then is used to design a feedback controller of RWMs. Some examples of application to the ITER geometry are reported.

Keywords: Resistive Wall Modes, 3D conducting structures
PACS: 52.35.Py, 28.52.Av, 52.55.Fa

INTRODUCTION

Surrounding the plasma with a sufficiently close conducting structure, it is possible to slow the growth rate of kink-like instabilities down to electromagnetic times. Indeed, the eddy currents induced in such conducting structures have a stabilizing effect, but they tend to decay, being the conductivity of the conducting wall finite, giving rise to the so-called Resistive Wall Modes (RWM).

Such modes are receiving an increasing attention, in view of their importance in present-day and future devices, like ITER, in setting limits in terms of achievable normalized beta. For this reason, it is of fundamental importance to make reliable predictions about the RWM stability boundary and to develop models which can be used for the design of an effective active control of such modes.

However, some open issues still remain in RWM modelling. One is the estimate of the stabilization effects due to plasma rotation and dissipation [1]. Another is the evaluation of the effects of the complex three-dimensional conducting structures surrounding the plasma [2, 3]; this effect is investigated in the present paper.

In particular, the CarMa code [4, 5, 6] is used to analyze configurations in which the three-dimensional effects may provide a significant contribution to the overall stability properties, from the point of view both of quantitative estimates of growth rates and of the interpretation of the RWM spectrum.

CP1069, *Theory of Fusion Plasmas, Joint Varenna-Lausanne International Workshop*
edited by X. Garbet, O. Sauter, and E. Sindoni

THE NUMERICAL MODEL

The CarMa code is described in details in [4, 5, 6]. It has been validated experimentally on the RFX-mod device [7]; its approach has been demonstrated analytically in [8-9]. Here we report only the main points.

The first assumption made is to neglect plasma mass, which is a very good approximation since the RWM growth time is typically much slower than the Alfvén time. Secondly, we disregard plasma rotation; this corresponds to a worst case assumption, since plasma flow has a stabilizing effect. In addition, it is not clear if in next-generation devices, including ITER, the rotation will give a significant contribution to the stabilization of RWMs [10].

As a consequence of these assumptions, the plasma reacts instantaneously (i.e. with no inertia) to external excitations (e.g. magnetic field perturbations).

In the following, we will assume a single toroidal mode $n = 1$ in the plasma. This is not a limitation, since the CarMa code can easily deal with multimodal coupling which can arise even in the linear case thanks to the three-dimensional conducting structure surrounding the plasma [7].

A surface S is chosen, in between the plasma and the conducting structures. The plasma (instantaneous) response to a given magnetic flux density perturbation on S is computed as a plasma response matrix, solving the linearized ideal MHD equations using the MARS-F code [11]. The currents induced in the 3D structures by plasma are described using a volumetric time-domain integral formulation of the eddy currents equations [12], which requires a finite elements discretization of the conducting structures only.

The effect of 3D structures on plasma is evaluated by computing the magnetic flux density on S due to 3D currents. The currents induced by plasma on the conducting structures are computed via an equivalent surface current distribution on S providing the same magnetic field as plasma outside S.

Let V_c be the conducting domain surrounding the plasma, which is discretized via a finite elements mesh. A part of this domain consists of active coils fed through a number of equipotential electrodes S_k with voltage V_k. We give a weak form of Ohm's law with the Galerkin approach, using as test function and basis functions the edge elements $\mathbf{N}_j$ related to the j-th edge of the mesh.

The overall mathematical model can be expressed as [6]:

$$\underline{\underline{L}}^{*} \frac{d\underline{I}}{dt} + \underline{\underline{R}}\,\underline{I} = \underline{\underline{F}}\,\underline{V} \tag{1}$$

where $\underline{I}$ is the vector made by the discrete degrees of freedom (DoF) representing the 3D current density $\mathbf{J}$ in the conducting structure as

$$\mathbf{J} = \sum_k I_k \nabla \times \mathbf{N}_k \tag{2}$$

The modified inductance matrix $\underline{\underline{L}}^{*}$ is a fully populated square matrix defined as:

$$\underline{\underline{L}}^{*} = \underline{\underline{L}} + \underline{\underline{X}} \tag{3}$$

$$L_{i,j} = \frac{\mu_0}{4\pi} \int_{V_c} \int_{V_c} \frac{\nabla \times \mathbf{N}_i(\mathbf{r}) \cdot \nabla \times \mathbf{N}_j(\mathbf{r}')}{|\mathbf{r} - \mathbf{r}'|} dV dV' \tag{4}$$

where $\underline{\underline{X}}$ is an additional term due to the presence of the plasma [6].

The resistance matrix $\underline{\underline{R}}$ is a sparse square matrix:

$$R_{i,j} = \int_{V_c} \nabla \times \mathbf{N}_i \cdot \underline{\underline{\eta}} \cdot \nabla \times \mathbf{N}_j dV \tag{5}$$

where $\underline{\underline{\eta}}$ is the resistivity tensor, while the matrix:

$$F_{i,j} = -\int_{S_j} \nabla \times \mathbf{N}_i \cdot \hat{\mathbf{n}} dS \tag{6}$$

describes the effect of voltage feeding of electrodes with normal **n**.

Simple manipulations of eq. (1) lead to

$$\frac{d\underline{I}}{dt} = \underline{\underline{A}}\underline{I} + \underline{\underline{B}}\underline{V}. \tag{7}$$

Introducing the vector made of magnetic field perturbations $\underline{y}$ at given points, we have also [6]:

$$\underline{y} = \underline{\underline{C}}\underline{I}. \tag{8}$$

Equations (7)-(8) define a state-space system which represent the evolution of the 3D currents in the structure taking into account the presence of a plasma.

FEEDBACK CONTROL OF RWM

Having the model described in the previous section, we can use the tools of control theory to study feedback stabilization of RWM by means of suitable actuators (i.e. non-axisymmetric saddle coils).

Best Achievable Performances

Considering n=1 unstable RWMs, the matrix $\underline{\underline{A}}$ in equation (7) has a pair of unstable eigenvalues $\alpha \pm j\omega$ $(\alpha > 0, \omega \geq 0)$, corresponding to unstable eigenmodes that are shifted of $\pi/2$ in the toroidal direction [4, 5, 6]. These modes must be stabilized by using the available control coils, which are voltage driven by suitable power supplies.

The voltage and currents limits of the power supplies constraint the amplitude of the maximum perturbations which can be recovered. A method to estimate such maximum perturbations is the evaluation of the null controllable region [13] of system (7) when the power supplies are subject to a given maximum voltage constraints. Hence, we assume that each component V_i of vector $\underline{V}$ is admissible when it satisfies the inequalities: $-V_{Mi} \leq V_i \leq V_{Mi}$, where V_{Mi} is the maximum voltage available on the i-th power supply.

An initial 3D current distribution $\underline{I}_0$ *is said to be null controllable, if there exists a finite time* t_f *and an admissible control voltage law* $\underline{V}(t)$ *such that the state trajectory* $\underline{I}(t)$ *of the system (7) satisfies* $\underline{I}(0)=\underline{I}_0$, $\underline{I}(t_f)=0$. *The set of all null controllable states is called the null controllable region of the system (7).*

By a suitable state space transformation $\underline{x} = \underline{\underline{S}}\,\underline{I}$, system (7) can be rewritten as follows:

$$\frac{d}{dt}\begin{bmatrix} x_1 \\ x_2 \\ \underline{x}_s \end{bmatrix} = \begin{bmatrix} \begin{bmatrix} \alpha & -\omega \\ \omega & \alpha \end{bmatrix} & \underline{\underline{0}} \\ \underline{\underline{0}} & \underline{\underline{A}}_s \end{bmatrix} \begin{bmatrix} x_1 \\ x_2 \\ \underline{x}_s \end{bmatrix} + \begin{bmatrix} \underline{\underline{B}}_u \\ \underline{\underline{B}}_s \end{bmatrix} \underline{V}. \tag{9}$$

The $n_s \times n_s$ matrix $\underline{\underline{A}}_s$ contains the stable modes of system (7). The null controllable region of systems (7) and (9) are isomorphic under the transformation $\underline{\underline{S}}$, so it possible to work directly with representation (9). A procedure to evaluate this null controllable region, outlined in [13], is based on solving a suitable optimal control problem for the reduced order system:

$$\frac{d}{dt}\begin{bmatrix} x_1 \\ x_2 \end{bmatrix} = \begin{bmatrix} \alpha & -\omega \\ \omega & \alpha \end{bmatrix} \begin{bmatrix} x_1 \\ x_2 \end{bmatrix} + \underline{\underline{B}}_u \underline{V}. \tag{10}$$

which contains only the two unstable modes.

In particular, let $\underline{\underline{P}}_e$ be the solution of the following Riccati equation:

$$\begin{bmatrix} \alpha & -\omega \\ \omega & \alpha \end{bmatrix}^T \underline{\underline{P}}_e + \underline{\underline{P}}_e \begin{bmatrix} \alpha & -\omega \\ \omega & \alpha \end{bmatrix} + \varepsilon \underline{\underline{I}} + \underline{\underline{P}}_e \underline{\underline{P}}_e = 0, \tag{11}$$

and

$$\underline{\underline{K}}_{e,\gamma} = -\gamma \underline{\underline{B}}_u^T \underline{\underline{P}}_e, \tag{12}$$

with γ and ε being two positive scalars sufficiently large ($\gamma \to \infty$) and small ($\varepsilon \to 0$), respectively. The null controllable region of system (9) can be obtained by evaluating the stability region guaranteed by the state feedback control law:

$$V = \mathrm{sat}\left(\underline{\underline{K}}_{e,\gamma} \begin{bmatrix} x_1 \\ x_2 \end{bmatrix} \right), \tag{13}$$

where sat(.) is a vector of saturation functions:

$$\mathrm{sat}_i(x) = \begin{cases} V_i & \text{if} \quad x > V_i \\ x & \text{if} \quad -V_i \le x \le V_i \\ -V_i & \text{if} \quad x < -V_i. \end{cases} \tag{14}$$

This evaluation can be performed by means of simulations. It is worth to notice that the control law (13) cannot be implemented in practice, since the components x_1 and x_2, along the unstable eigenvectors are not directly measurable.

Once the null controllable region has been evaluated, it is possible to characterize the maximum allowable perturbations as initial (i.e. at $t = 0$) perturbations of the magnetic fields measured by the sensors, using the output mapping in equation (8). These maximum initial perturbations define the so-called Best Achievable Performances (BAP).

The procedure for the estimation of the best achievable performance can be modified so as to take into accounts the limits on the currents flowing in the active coils. Let S_c denotes the null controllable region; we define $S_{ca} \subseteq S_c$ as *the set of the initial 3D current distribution* $\underline{I}_0$ *for which there exists a finite time* t_f *and an admissible control voltage law* $\underline{V}(t)$ *such that the state trajectory* $\underline{I}(t)$ *of the system (1)*

satisfies $\underline{I}(0)=\underline{I}_0$, $\underline{I}(t_f)=0$, *and* $-I_{Mi} \leq I_{acti}(t) \leq I_{Mi}$, *for all* $0 \leq t \leq t_f$, where I_{acti} denotes the current flowing in the *i*-th active circuit.

The analytical evaluation of the set S_{ca} is a very complex task, so that we resort to a simplified procedure allowing us to obtain a subset $S_{ce} \subseteq S_{ca}$. This procedure is based on shrinking the set S_c until the constraint on the active currents are not satisfied. Again this evaluation can be performed off-line by means of numerical simulations.

Controller design

The controller design is based on the following requirements.

1) Obtain a closed loop null controllable region as close as possible to the null controllable region determined by using the procedure outlined in the previous section;
2) Allow to recover from a disturbance (modelled as an initial condition lying on the unstable plane) as soon as possible, compatibly with the constraints on the active coil voltages and currents;
3) To avoid to generate a $n \neq 1$ magnetic field.

The feedback controller scheme is depicted in Fig. 1. The "Plasma/circuit model" is represented by equations (7)-(8), while the transformation matrices $\underline{\underline{T}}_{IN}$ and $\underline{\underline{T}}_{OUT}$ are determined as follows. The matrix $\underline{\underline{T}}_{IN}$ allows to evaluate the active voltage $\underline{V}$ from the $n=1$ Fourier components of a spatially sinusoidal voltage waveform $\underline{V}_1$, while the matrix $\underline{\underline{T}}_{OUT}$ transform the magnetic field spatial distribution $\underline{y}$ to its $n=1$ Fourier components $\underline{y}_1$.

The controller $\underline{\underline{K}}$ is a dynamic multivariable controller designed by using the LQG technique [14]. A balanced truncation technique [14] is used to obtain a sufficiently low order controller. The main idea is to evaluate the importance of the single states to the input-output map of the system to be reduced. In order to do this, we compute the observability gramian $\underline{\underline{Y}}_O$ and the controllability gramian $\underline{\underline{X}}_C$ of the system. It can be shown that there exist a matrix $\underline{\underline{T}}$ (called balanced transformation) such that:

$$\underline{\underline{T}}\,\underline{\underline{X}}_C\,\underline{\underline{T}}^T = \underline{\underline{T}}^{-1}\,\underline{\underline{Y}}_O\left(\underline{\underline{T}}^{-1}\right)^T = \Sigma . \qquad (15)$$

where Σ is a diagonal matrix whose diagonal entries h_i are called the Henkel Singular Values. The quantities h_i are a quantitative measure of both observability and controllability, and hence provide an indication of the importance of the corresponding state to the input-output map. Consequently, we can reduce the order of the system only to those states which significantly contribute to the input-output map; when doing this reduction, also an error estimate is available.

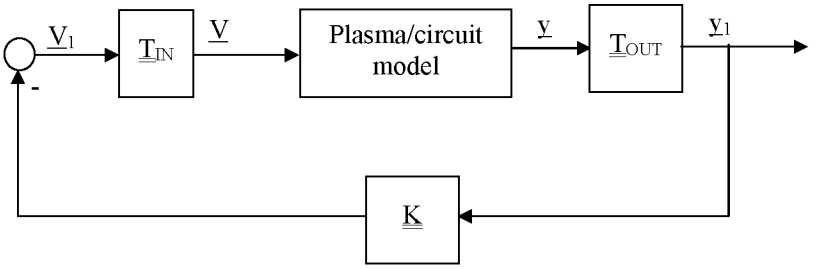

FIGURE 1. RWM feedback controller scheme.

RESULTS

In this section we report some results obtained on the ITER geometry. Both open-loop and closed-loop analysis have been carried out.

Growth rate calculation

The reference geometry is reported in Fig. 2. A high level of geometrical details have been included in the model: double shell vessel, nested port extensions, outer triangular support (the copper cladding has been represented using an equivalent resistivity), internal active coils. The latter are 27, arranged over nine toroidal sectors; the geometrical parameters used refer to the so-called VAC02-A option. In fact, these coils are primary intended for ELM control; in this paper we analyze their possible use also for RWM control.

Two sets of different ITER equilibria have been considered: non-smoothed equilibria (reference) and smoothed ones, in which the plasma region around the X-point has been smoothed, with a consequent diminution of the edge value of safety factor q – the rest of the q profile has been kept practically unchanged.

Figure 3 reports the growth rates of the n = 1 RWM for various values of normalized beta β_N, assuming that the active coils are left open-circuited. Evidently, the non-smoothed equilibria are substantially more stable for similar values of β_N, due to the higher q value at the plasma edge.

In the same figures we also report the values of the growth rates obtained also using an axisymmetric mesh with the same poloidal cross section (i.e. with no port extensions) and using a mesh in which ports are replaced by pure holes – this is the simplest 3D modeling that one can think of [15]. Evidently, the purely axisymmetric assumption is very optimistic, while considering holes is heavily pessimistic. Hence, a correct 3D modeling of geometrical details (port extensions, in this case) may be crucial for the analysis of RWM.

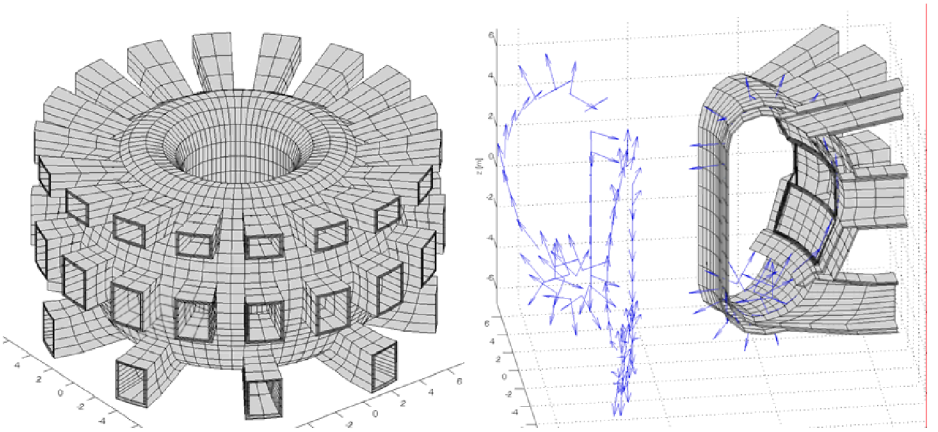

(a) (b)

FIGURE 2. Modeled ITER geometry: (a) overall view, (b) cutaway diagram showing internal control coils and location and orientation of simulated magnetic measurements

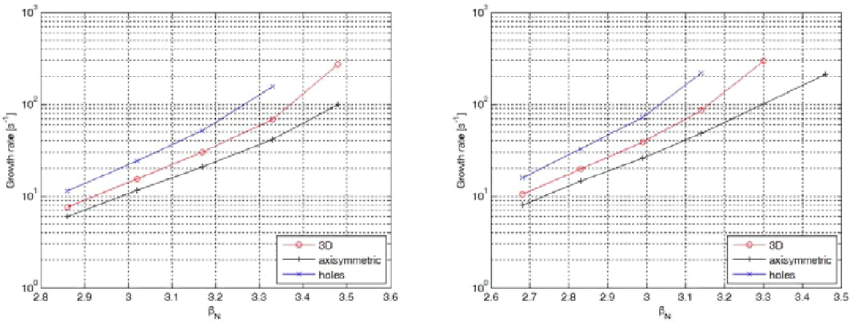

(a) (b)

FIGURE 3. RWM growth rates as a function of normalized beta for (a) non-smoothed and (b) smoothed ITER equilibria

Best Achievable Performances

We have computed the best achievable performances for the non-smoothed equilibrium with β_N = 3.17 (growth rate with only passive structures 30.0 s^{-1}), assuming the following voltage and current limits for the ELM control coils:

a) No ELM control

V_{max} = 75 V, I_{max} = 20 kA (upper and lower coils), I_{max}=13 kA (middle coil)

b) ELM control active

V_{max} = 28 V, I_{max} = 250A

Indeed, when ELM control is switched off the full performances of the actuators are available for RWM control; conversely, when it is active, ELM control needs a substantial part of the available voltage and current.

We define the quantities y_1 and y_2 as:

$$y_1(t) = \frac{2}{N}\sum_{k=1}^{N} B_k(t)\cos(\phi_k), \qquad y_2(t) = \frac{2}{N}\sum_{k=1}^{N} B_k(t)\sin(\phi_k) \tag{16}$$

where $B_k(t)$ are $N=18$ measurements of the vertical magnetic field in the outboard region at equally spaced toroidal angles φ_k.

In Figure 4 we report the results; the perturbations corresponding to points in the interior of the polygons can be stabilized with the given voltage and current limits. It can be noticed that perturbations up to a few tens of mT can be stabilized when full performance is available for RWM control. Conversely, when ELM control is off only substantially smaller perturbations (of the order of fractions of mT) can be stabilized.

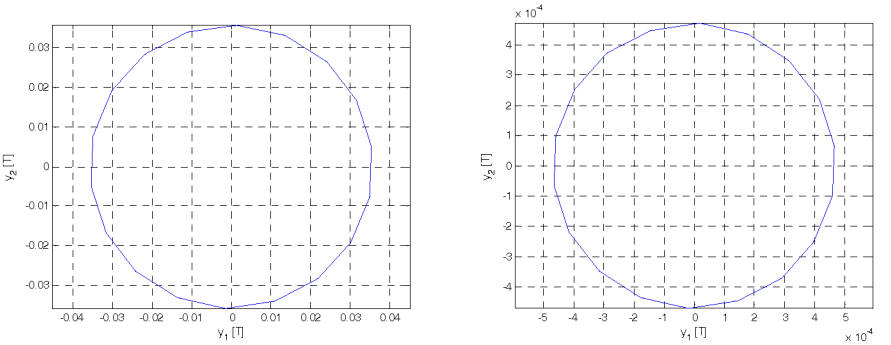

FIGURE 4. Best Achievable Performances: (a) ELM control not active and (b) ELM control on

Feedback controller simulations

The controller has been designed to counteract perturbations along the unstable eigenmodes of a reduced order model. However, it has been successfully verified on the full model (i.e. with no order reduction), imposing a random initial condition on the whole state (hence both on unstable and on stable modes).

Figures 5 and 6 show the required current in the active control coils, while Figure 6 shows the magnetic field perturbations at the locations reported in Fig. 1. These quantities are reported for the equilibrium with β_N = 3.17 (growth rate with only passive structures 30.0 s^{-1}), for both cases a) and b) mentioned above (ELM control active or not). Similar results can be obtained for the configurations with slower growth rate.

We can note the following.

- The controller is able to stabilize a set of different equilibria, although it has been designed on the most unstable with no particular requirements on robustness.
- The maximum magnetic field displacement is of the same order of the Best Achievable Performance shown in the previous section; this means that the controller is not far from the maximum achievable.
- The actual limiting factor on performance is the current limit.
- If the ELM control is active, only very small perturbations can be stabilized (fractions of mT in terms of magnetic field).

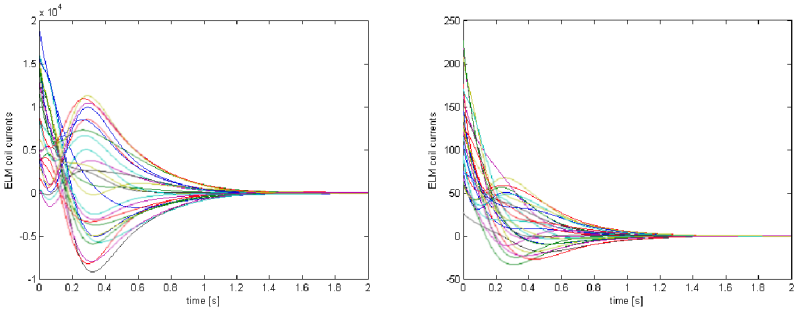

(a) (b)

FIGURE 5. Active coil currents with RWM feedback controller: (a) ELM control not active and (b) ELM control on

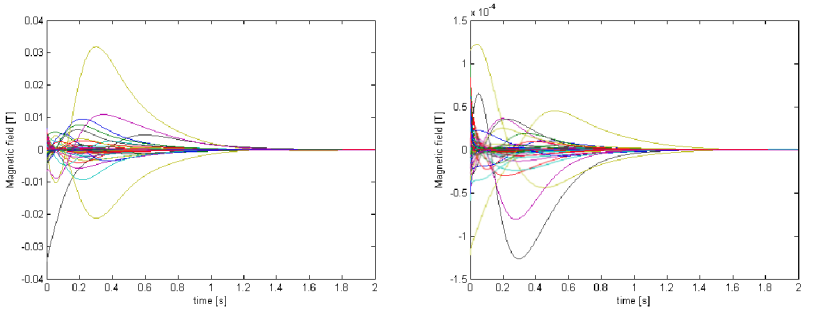

(a) (b)

FIGURE 6. Magnetic field perturbations with RWM feedback controller: (a) ELM control not active and (b) ELM control on

CONCLUSIONS

In this paper we have illustrated how Resistive Wall Modes can be analyzed and stabilized using a mathematical model taking into account three-dimensional effects of the conducting structures surrounding the plasma. To this purpose, the CarMa code has been used. Thanks to properties of the resulting model, the Best Achievable Performances can be estimated and a feedback controller can be designed. The ITER geometry with a high level of geometrical details has been studied.

ACKNOWLEDGMENTS

The authors acknowledge useful discussions with Prof. R. Albanese, Prof. G. Rubinacci and Dr. A. Portone, who also provided the geometrical data of ITER.

This work was supported in part by CREATE and Italian Ministry of University and Research under PRIN grant.

REFERENCES

1. A. Bondeson, D. J. Ward, *Phys. Rev. Lett.* **72** 2709 (1994)
2. J. Bialek, A. H. Boozer, M.E. Manuel and G.A. Navratil, *Phys. Plasmas* **8** 2170-80 (2001)
3. E. Strumberger, P. Merkel, M. Sempf, and S. Günter, *Phys. Plasmas*, **15** 056110 (2008)
4. F. Villone et al., *34th EPS Conference on Plasma Phys.* Warsaw, 2 - 6 July 2007 ECA Vol.**31F**, P-5.125 (2007)
5. R. Albanese, Y. Q. Liu, A. Portone, G. Rubinacci, and F. Villone, *IEEE Trans. Magn.* **44**, 1654 (2008)
6. A. Portone, F. Villone, Y. Q. Liu, R. Albanese, and G. Rubinacci, *Plasma Phys. Controlled Fusion* **50**, 085004 (2008)
7. F. Villone, Y. Q. Liu, R. Paccagnella, T. Bolzonella, and G. Rubinacci, *Phys. Rev. Lett.* **100**, 255005 (2008)
8. Y. Q. Liu, R. Albanese, A. Portone, G. Rubinacci, and F. Villone, *Phys. Plasmas* **15** 072516 (2008)
9. V. D. Pustovitov, *Plasma Phys. Controlled Fusion* **50**, 105001 (2008)
10. Y.Q. Liu, et al., *Nucl. Fusion* **44**, 232 (2004)
11. Y. Q. Liu and A. Bondeson, *Phys. Rev. Lett.* **84** 907 (2000)
12. R. Albanese, G. Rubinacci, *IEE Proc.* Part A **135** 457–462 (1988)
13. T. Hu, Z. Lin, *International Journal of Robust and Nonlinear Control*, **11**, 555 (2001)
14. B.D.O. Anderson, J.B. Moore, *Optimal Control*, Prentice Hall, 1990
15. F. Villone et al., *35th EPS Conference on Plasma Phys.* Hersonissos, 9 - 13 June 2008 ECA Vol.**32**, P-2.080 (2008)